

# In-Vivo Magnetic Field Correlation Imaging of Human Brain at 3 Tesla

A. Ramani<sup>1</sup>, J. H. Jensen<sup>1</sup>, K. R. Kaczynski<sup>2</sup>, J. A. Helpert<sup>1,3</sup>

<sup>1</sup>Center for Biomedical Imaging, Department of Radiology, New York University School of Medicine, New York, NY, United States, <sup>2</sup>Siemens Medical Solutions, New York, NY, United States, <sup>3</sup>Center for Advanced Brain Imaging, The Nathan S. Kline Institute, Orangeburg, New York, United States

**INTRODUCTION:** As water molecules diffuse through a tissue under the influence of a strong uniform applied magnetic field, typically encountered in a MRI scanner, they sample a complex landscape of field inhomogeneities generated by variations in magnetic susceptibility. These susceptibility variations arise not only from macroscopic structures, such as air cavities and large veins, but also from microscopic structures, such as capillaries and iron-rich cells. The field inhomogeneities experienced by water molecules can be quantified by their magnetic field correlation (MFC). This is formally defined by Eqn. [1]:

$$K(t_2 - t_1) = \langle B(t_2)B(t_1) \rangle \quad [1]$$

where  $B(t)$  is the field shift, relative to the uniform background field, for a particular water molecule at a time  $t$  and with the angle brackets indicating an averaging over all the molecules within a given region of interest (1). The MFC can be calculated using an asymmetric spin echo (ASE) sequence (1). In this abstract, we have demonstrated the feasibility of MFC imaging at 3 Tesla by showing in-vivo MFC images of the human brain and have also correlated MFC values with putative iron concentrations in specific brain regions. This technique may provide important information in the assessment of neurological disorders with associated iron abnormalities, such as Parkinson's disease, Alzheimer's disease, Hallervorden-Spatz syndrome etc.

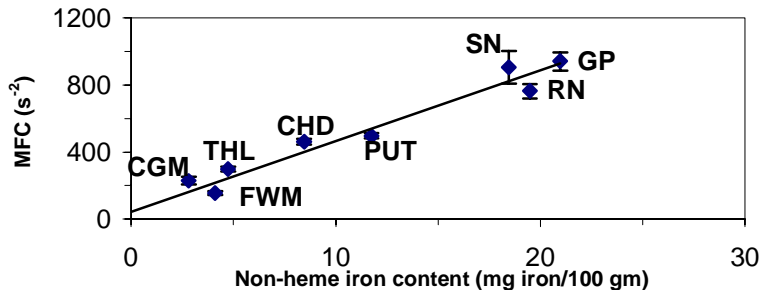
**THEORY:** Consider an asymmetric SE sequence in which the 180° refocusing pulse is shifted by a time  $t_s$  from its standard position (i.e.,  $t_s = 0$  corresponds to a conventional SE sequence). If the field inhomogeneities are not too large, then we can write:

$$S(t_s) = S_0 \exp \left[ -2t_s^2 \gamma^2 K \left( \frac{TE}{2} \right) \right] \quad [2]$$

where  $S$  is the signal intensity,  $TE$  is the echo time, and  $\gamma$  is the proton gyromagnetic ratio (1, 2). MFC maps are generated by fitting the signal intensities as a function of the pulse shifts on a pixel-by-pixel basis, to Eqn. [2]. The validity of this equation for biological tissues has been confirmed both with Monte Carlo simulations (1) and suspensions of yeast cells containing a paramagnetic contrast agent (2).

**METHODS:** ASE images were acquired using a segmented EPI sequence from six normal volunteers on a Siemens Allegra 3 Tesla scanner. Four echo times were used ( $TE = 26, 32, 50, 69$  ms) with five refocusing pulse shifts (0.0, 3.0, 6.0, 9.0, and 12.0 ms) for each TE. Using a repetition time of 2000 ms, FOV of 230 mm, 10 averages and a matrix size of 128 x 128, MFC data was acquired from 20 slices (1.8 mm thick). Signal intensities were measured from brain regions including putamen (PUT), globus pallidus (GP), substantia nigra (SN), thalamus (THL), caudate head (CHD), frontal white matter (FWM) and cortical gray matter (CGM). MFC maps were extracted as explained above. The transverse relaxation rate  $R_2$  was calculated by fitting the signal intensities (corresponding to the four TEs) as a function of TE. Single-shot diffusion-weighted EPI was also performed using the following parameters: TR 2000 ms, TE 88 ms, slice thickness 1.2 mm with 10 averages. SE images were obtained using three  $b$  values (300, 600 and 900 seconds/mm<sup>2</sup>), comprised of 128x96 pixels and covered an FOV of 230 mm from which ADC maps were extracted.

**RESULTS:** Figure 1(a) shows a typical MFC map acquired at an echo time of 50 ms. The most interesting structures are near the center of the image and are associated with the globus pallidus (short arrows), a region known for its high iron content. Features corresponding to blood veins and an artifact due to the sinus air cavity (long arrow) are also apparent. Figures 1(b) and 1(c) are  $R_2$  and ADC maps produced at the same slice location. The MFC was found to decrease with increasing TE, reflecting the diffusion of water molecules through microscopic gradients. Table 1 shows regional MFC, ADC and  $T_2$  values in 6 subjects. It is clear the regional variation in MFC values is higher than both ADC and  $T_2$  values. Figure 2 shows a strong correlation ( $r = 0.975$ ) between MFC and established age-related iron concentrations (3), suggesting that MFC imaging is sensitive to iron-induced differences in brain-tissue susceptibility.



| Region | MFC (s <sup>-2</sup> ) | ADC (μm <sup>2</sup> /ms) | T <sub>2</sub> (ms) |
|--------|------------------------|---------------------------|---------------------|
| GP     | 941.13 ± 54.2          | 0.789 ± 0.05              | 40.95±1.43          |
| SN     | 905.91 ± 96.7          | 0.771 ± 0.07              | 46.06±2.06          |
| RN     | 763.87 ± 43.2          | 0.775 ± 0.06              | 43.32±2.23          |
| PUT    | 505.54 ± 25.8          | 0.793 ± 0.05              | 53.03±2.98          |
| CHD    | 452.98 ± 26.7          | 0.805 ± 0.04              | 58.25±1.22          |
| THL    | 298.88 ± 18.7          | 0.757 ± 0.05              | 56.44±2.94          |
| CGM    | 227.8 ± 24.0           | 0.814 ± 0.09              | 76.09±3.65          |
| FWM    | 154.19 ± 27.1          | 0.904 ± 0.07              | 58.25±4.21          |

**Figure 2.** Quantitative regional MFC measurements plotted versus published iron concentrations.  $MFC = (41 \pm 3) * (\text{Iron content}) + 42 \pm 18$

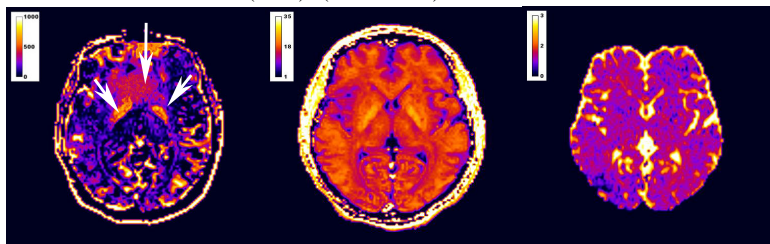


**Table 1:** Regional MRI estimates for the MFC, ADC and  $T_2$  obtained in-vivo from nine brain structures in 6 subjects

**Figure 1.** (a) MFC map at TE=50 ms. The scale bar indicates the magnitude of  $\gamma^2 K(TE/2)$  in units of s<sup>-2</sup>. (b,c)  $R_2$  and ADC maps of the same subject at the same slice location.

**ACKNOWLEDGMENTS:** Funded by NIH grant R21 EB003305-01 from the NIBIB and by grants from the Institute of Study of Aging and the Werner Dannheisser Testamentary Trust.

**REFERENCES:**

- Jensen JH, Chandra R. *Proc Intl Soc Magn Reson Med*; **10**:2297 (2002).
- Jensen JH, Johnson G, Chandra R, Helpert JA. *Proc Intl Soc Magn Reson Med*; **11**:1120 (2003).
- Hallgren B, Sourander PJ. *Neurochem*. **3**: 41-51: (1958).